A Letters Journal Exploring
the Frontiers of Physics

OFFPRINT

The role of wetting heterogeneities in the meandering instability of a partial wetting rivulet

S. Couvreur and A. Daerr

EPL, **99** (2012) 24004

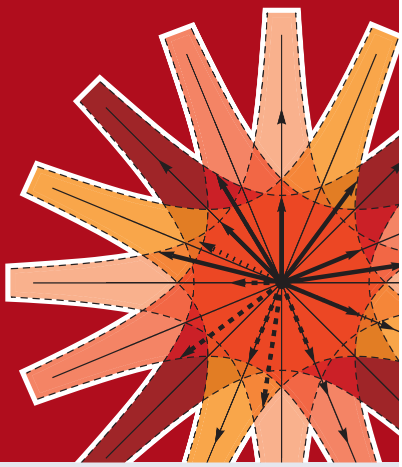

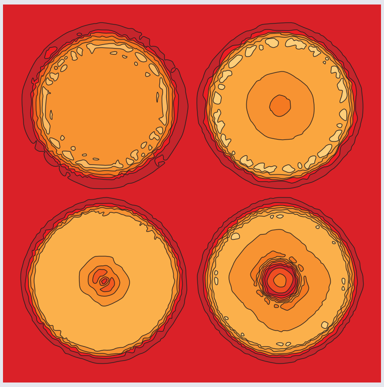

Biaxial strain on lens-shaped quantum rings of different inner radii, adapted from **Zhang *et al*** 2008 EPL **83** 67004.

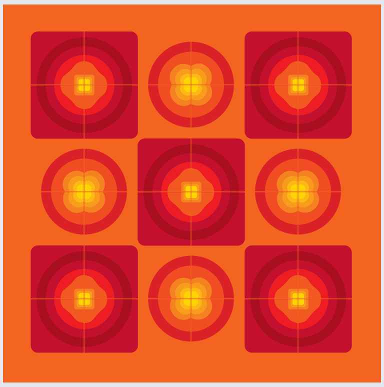

Artistic impression of electrostatic particle–particle interactions in dielectrophoresis, adapted from **N Aubry and P Singh** 2006 *EPL* **74** 623.

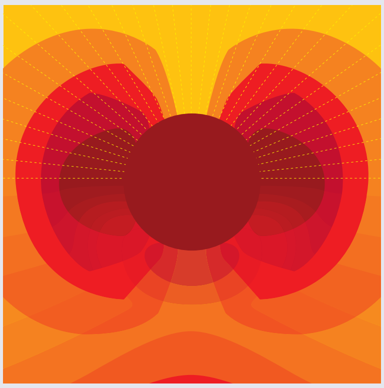

Artistic impression of velocity and normal stress profiles around a sphere that moves through a polymer solution, adapted from **R Tuinier, J K G Dhont and T-H Fan** 2006 *EPL* **75** 929.

Image: Ornamental multiplication of space-time figures of temperature transformation rules (adapted from T. S. Bíró and P. Ván 2010 *EPL* **89** 30001; artistic impression by Frédérique Swist).

A Letters Journal Exploring
the Frontiers of Physics

July 2012

EPL, **99** (2012) 24004
doi: 10.1209/0295-5075/99/24004

www.epljournal.org

The role of wetting heterogeneities in the meandering instability of a partial wetting rivulet

S. Couvreur[(a)] and A. Daerr

Univ Paris Diderot, Sorbonne Paris Cité, Matière et Systèmes Complexes - 75013, Paris, France, EU

received 10 April 2012; accepted in final form 27 June 2012
published online 27 July 2012

PACS 47.20.Ma – Interfacial instabilities (*e.g.*, Rayleigh-Taylor)
PACS 47.55.np – Contact lines
PACS 47.20.Qr – Centrifugal instabilities (*e.g.*, Taylor-Couette flow)

Abstract – Rivers are subject to a meandering instability caused by sediment transport. A liquid rivulet on an inclined plate in partial wetting conditions exhibits a similar instability at sufficiently high flow rates. It takes a sinuous shape: curves become bigger and bigger, growing by inertia from contact line defects. Meanders are eventually stationary because of the pinning force. The way the initial rivulet is created has consequences on the contact line's shape. We run experiments to study how the critical flow rate depends on initial conditions. We measure a strong dependence, in particular by modifying the initial state from which meanders are growing: it shows that the pinning force plays the main role in the meandering instability. This is in contrast with the previous approach in which only a balance is considered between inertia and a line tension of capillary origin. Because of wetting hysteresis, rivulets have the capacity to deform without any movement of the contact line. We show that the rivulet deforms in response to the centrifugal force. This deformation also helps us to understand how the critical flow rate depends on the initial rivulet shape.

Meandering instability often refers to geophysics and river meandering [1–3]. Although the mechanism is still not well understood, we know it is linked to soil erosion. However, sediment transport is not a necessary condition for meanders: a similar instability exists for a liquid rivulet flowing down an inclined partially wetting plate [4–10].

For small flow rates, the water flows following by gravity along a straight line (fig. 1(a)). Note that the path is not perfectly straight, but that the contact line has irregularities due to heterogeneities in the wetting properties of the substrate. These perturbations are small, at most of the order of the width of the rivulet. When exceeding a critical flow rate, meandering is observed: the rivulet is destabilized and meanders grow. After a sometimes long transient regime (1 to 100 minutes), meanders become stationary (fig. 1(b)). The typical lateral excursion of the meandering path is large compared to the rivulet width. Finally, above a second critical flow rate meanders do not stabilize anymore and the rivulet often breaks down (fig. 1(c)).

The mechanism by which the straight path becomes unstable, and by which meanders form, is not entirely clear. It has been suggested that the instability results from a competition between inertia and capillarity: liquid flowing along a small deformation of the rivulet path will

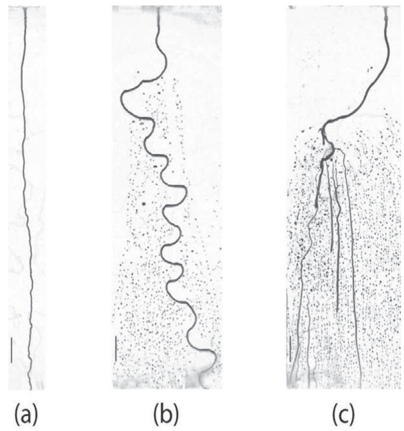

Fig. 1: A liquid rivulet flows down a partially wetting substrate. For increasing rates, several regimes are observed (scale: black line = 5 cm). (a) The rivulet is straight; (b) the shape is sinuous and stationary meanders are created; (c) unstationary regime, the rivulet often breaks down.

(a)E-mail: stephanie.couvreur@univ-paris-diderot.fs

experience centrifugal forces, which exceed the stabilising surface tension forces for high enough flow rates, and tend to amplify the initial deformation of the path [5,11]. In the case of a liquid film flowing between two solid walls in total wetting conditions, this competition of forces was indeed shown recently to result in a linear instability, provided the velocity of the liquid *relative* to the perturbation is used to evaluate the inertial term[12]. In the presence of pinned contact lines, however, this linear instability is suppressed. A local perturbation may cause a rivulet cross-section to oscillate around its equilibrium shape, but eventually viscous damping will attenuate the perturbation. Because a finite amplitude is required to reach the critical advancing or receding contact angle on either side, and thus to de-pin the contact line, an infinitesimal perturbation will not suffice to trigger meandering.

The nature of the meandering instability in partial wetting conditions has been debated also by Birnir *et al.* [13], who reported an experimental set-up (water-glycerol mixtures on acrylic substrates) where no meandering was observed. They recover meanders only while they modulate the flow rate at the injection, and conjecture that meandering requires such flow rate fluctuations. The fact that several of the preceeding studies [9,14] report meandering despite using the same constant level tank to minimize flow rate fluctuations, is not explained. Birnir *et al.*'s theoretical model, on the other hand, relies on spatial noise to produce meandering paths. This noise is introduced phenomenologically, and needs to have particular properties (white noise will apparently not do), making it hard to learn anything about the instability from the model. We revisit the transition between the straight rivulet regime and the stationary meandering one experimentally, and focus on the role of contact line pinning and noise. We identify the importance of the initial rivulet shape on the meandering threshold, and offer a tentative explanation of contradicting observations in the literature.

Experimental set-up. – Liquid (water here) is injected on a vertical glass plate ($0.85\,\mathrm{m} \times 1.05\,\mathrm{m}$) at a very stable flow rate by means of a constant level tank. Different surface treatments are available to control the glass wetting properties, but we here focus on the case of a clean glass plate, without any coating, and maintained vertical. An appropriate optical set-up involving a large Fresnel lens is used to obtain pictures with a high contrast (fig. 2). Before every experiment, the glass is cleaned with ethanol and acetone and drops remaining from previous experiments are removed.

Results. – In previous studies, experiments were done for increasing flow rates and starting from zero. For a given plate slope, a single critical rate could be defined. We show that reality is a little more complex and starting from a non-zero flow rate leads to a higher critical flow rate. Indeed, we can prepare straight rivulets in different ways.

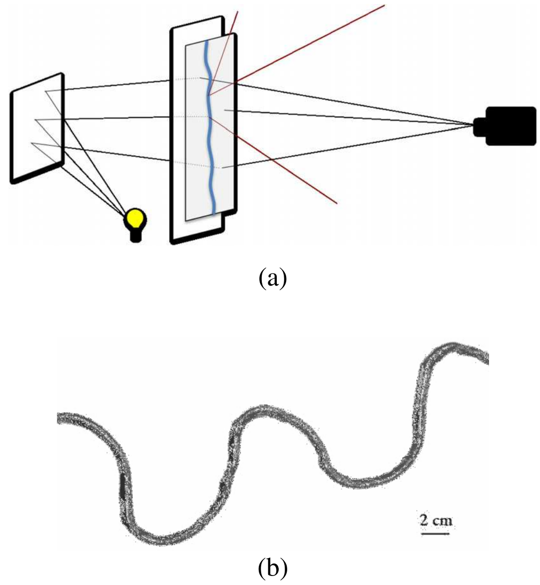

Fig. 2: (Colour on-line) The light source and the camera pupil are at optically conjugated positions of a 1-meter-focal convex Fresnel lens placed just below the glass plate. Without any water, the light rays through every point of the lens are focussed into the camera. The curved water/air interface of a flowing rivulet deviates light rays away from the camera entrance pupil. We obtain a contrasted picture with a light background and a completely black rivulet inside which the line of maximal thickness appears as a thin white line.

At every flow rate we can reach with our experimental set-up, even well into the meandering regime, we can straighten up the rivulet by forcing its path with a water squeeze bottle or a cotton bud put in contact with the liquid and progressively moved in the desired direction. The smoothness and the width of this straightened rivulet vary within a certain range, but the tendency is that bigger "preparation" rates will lead to smoother and larger rivulets. We now increase the flow rate further until the rivulet starts to meander. We observe that this new critical flow rate depends on the preparation flow rate.

In order to quantify the smoothness of the rivulet, we use image analysis to extract local curvatures of both contact lines, and average over both sides to define the local curvature of the rivulet. This curvature can be both positive and negative, and its mean is zero. A typical curvature C is calculated as the square root of the mean of the local curvature to the square, providing a good measure of the rivulet roughness.

In fig. 3, both the preparation flow rate Q_i and the associated critical flow rate Q_c are plotted as a function the root mean square (RMS) curvature C of the prepared straight rivulet. Despite some scatter, we can note two effects of bigger initial flow rates, at which the straight rivulet was prepared: on the one hand, rivulets tend to be smoother (that is to say their RMS curvature C is smaller). On the other hand, the critical flow rates for meandering

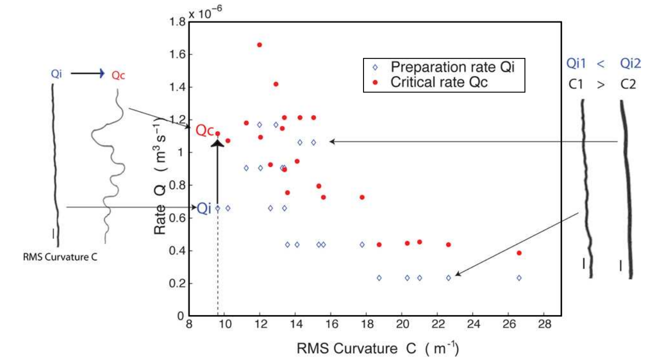

Fig. 3: (Colour on-line) Data showing the dependency of the critical meandering rate regarding preparation. For a straight rivulet at an initial rate Q_i (blue diamond), we measure the root mean square C of its curvature, which measures the roughness of the contact line. We then increase the flow rate and detect the critical meandering rate Q_c (red circle). The smaller the initial flow is, the rougher the contact line is and the bigger the root mean square curvature C is.

are higher. We will show that the two observations are linked, and that higher critical flow rates directly result from a lower curvature C. This highlights the importance of the initial conditions and the preparation of the initial rivulet.

As the contact line is rough, we consider a cross-section of the liquid rivulet (fig. 4) at a position where the rivulet path is bent in a perturbation with a radius of curvature R. Due to the constrained motion, the liquid is subjected to the centrifugal force which tends to destabilize the rivulet path. The surface tension and the pinning force act against this force and tend to stabilize. The faster the water flows, the higher the centrifugal force, and the more the rivulet section is deformed from its symmetric equilibrium shape. When it reaches a limit contact angle, the contact line moves. This corresponds to the critical flow rate at which meanders grow.

Model. – For a better understanding of this dependency, we model the flow inside the rivulet. We will show below that the increased critical flow rate is a consequence of the change in geometry, which determines the centrifugal forces: for higher preparation flow rates, inertia tends to smooth the contact line, the curvature decreases and perturbations felt by the flow are less sharp thus the critical meandering rate increases.

We consider a rivulet with a fixed width $2a$ in a small curve whose radius of curvature is R. The width of the rivulet is constant: experimentally, the width of the rivulet does not grow when increasing the flow rate. However, the section does increase, so that the angle at the contact line is related to the flow rate. Also, the rivulet shape is more and more deformed by inertial forces. When the deformation becomes such that the external contact angle reaches the limit advancing contact angle θ_a, the contact line moves and the meandering instability starts.

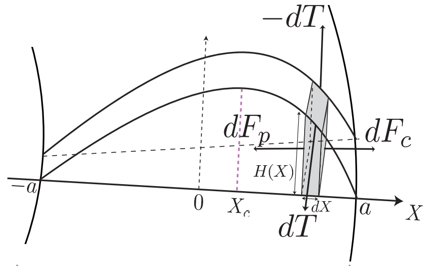

Fig. 4: The profile of a rivulet. We consider a force equilibrium on a column of fluid of height $H(X)$. Centrifugal $\mathrm{d}F_c$ and pressure $\mathrm{d}F_p$ forces are acting on the sides of the column (lateral surface tension terms are included in the pressure force). In a curved rivulet, the effective line tension $\mathrm{d}T$ due to the surface tension results in a $\mathrm{d}F_t$ force, when projected on the X direction.

We consider the forces per unit rivulet length acting on a column of fluid, in the limit of small slopes and neglecting gravity (fig. 4). The centrifugal force scales as

$$\mathrm{d}F_c = \rho H \frac{v^2}{R}\,\mathrm{d}X, \tag{1}$$

where ρ is the density, $H(X)$ is the height of the rivulet, $v(X)$ is a characteristic velocity of the liquid in the column, and R the local radius of curvature of the rivulet path. Because the free surface is curved both in the streamwise direction (with radius R) and in the direction transverse to the flow, we have two capillary force terms along X:

$$\mathrm{d}F_p = \gamma H H'''\mathrm{d}X, \qquad \mathrm{d}F_t = -\frac{\gamma}{R}\sqrt{1+H'^2}\,\mathrm{d}X, \tag{2}$$

where γ is the surface tension. The first term $\mathrm{d}F_p$ is due to Laplace pressure gradients which arise when the curvature transverse to the flow is not constant, *e.g.*, because the rivulet cross-section is deformed from its circular base shape (fig. 4). The second term $\mathrm{d}F_t$ results from the fact that the surface tension acts on the up-flow and down-flow sides of our column of fluid as an effective line tension $\mathrm{d}T$. For a curved rivulet path, this results in a normal force $\mathrm{d}F_t$ proportional to $1/R$, similar to the restoring force on a violin string.

Experimentally, the radius of curvature of the rivulet path is always larger than the rivulet half-width a. In that case the force term $\mathrm{d}F_t$ is negligible compared to $\mathrm{d}F_p$: $\mathrm{d}F_t$ is of the order $\gamma\,\mathrm{d}X/R$, while $\mathrm{d}F_p$ is of the order $\gamma\,\mathrm{d}X/a$. Furthermore, R can be considered independent of x.

We consider that the velocity profile of the liquid corresponds to a Poiseuille flow with $v \simeq \frac{g}{3\nu}H^2$, where ν is the viscous diffusion coefficient.

The force equilibrium reads, in non-dimensional variables $x = \frac{X}{a}$, $h = \frac{H}{a}$, a being one-half of the width of the rivulet:

$$h'''(x) = -\frac{a^6}{l_c^2\,\Lambda^3 R}h(x)^4, \quad \Lambda^3 = \frac{9\nu^2}{g}, \quad l_c = \sqrt{\frac{\gamma}{\rho g}}, \tag{3}$$

where l_c is the capillary length.

The centrifugal force tends to deform the rivulet toward the external side of the curve, breaking the symmetry.

The polynomial solution to 3rd order in x, assuming that the cross-sectional area of the rivulet is the same for the symmetric and the deformed rivulet, is

$$h(x) = \underbrace{\frac{\theta_s}{2}(1-x^2)}_{\text{symmetrical profile}} \left(1+\frac{1}{3}Ax\right), \tag{4}$$

$$A = \frac{L_0}{R}\frac{Q}{Q_0}, \qquad L_0 = \frac{a^6}{16 l_c^2 \Lambda^3}, \qquad Q_0 = \frac{32}{35}\frac{g}{24\nu}a^4. \tag{5}$$

θ_s is defined as the contact angle of the symmetrical parabolic base state. Assuming the Poiseuille flow, we can relate it to the flow rate Q:

$$Q = \frac{32}{35}\frac{g}{24\nu}a^4\theta_s^3 = Q_0\theta_s^3. \tag{6}$$

The prefactors are condensed into a typical flow rate Q_0, which depends only on the rivulet width $2a$.

The quantity A measures the deviation from the symmetrical profile. Again, the prefactors are condensed into a length L_0, which has no obvious physical meaning. When the rivulet get deformed by inertia, contact angles deviate from the contact angle θ_s, and their expression is deduced from eq. (4):

$$\theta(x=\pm 1) = \theta_s\left(1 \pm \frac{A}{3}\right). \tag{7}$$

Equation (7) gives us the two contact angles as a function of the flow rate, the width of the profile and the curvature radius of the perturbation considered. We postulate that the critical rate Q_c is reached when the critical advancing contact angle θ_a is reached on the outside of the bend, *i.e.*, $\theta(x=1)=\theta_a$. This is the case when

$$\frac{L_0}{R} = 3\left(\theta_a - \theta_s\right)\theta_s^{-4}. \tag{8}$$

A fit of the experimental data of this equation is presented in fig. 5. The fit has two parameters b and k defined as $L_0 \cdot C = 3k(b-\theta_s)\theta_s^{-4}$. The width of the rivulet is now taken into account (through L_0 and θ_s). The data points are not anymore dispersed like in fig. 3 but are lining up on a curve. As we work with high resolution pictures instead of high frame rate movies, we generally do not know which portion of the rivulet is the first to become unstable and grow into meanders. Therefore, we cannot measure the precise radius of curvature of the rivulet segment which first becomes unstable. Instead we calculate the RMS value C of the curvature at the preparation rate. This standard deviation of the curvature is expected to be proportional to the curvature of the most curved rivulet segment, so we introduce a parameter $k<1$ in the fit, which we expect and find to be of order one. The parameter b corresponds here to the limit advancing contact angle. We experimentally measure $\theta_a = 0.92 \pm 0.04$ which agrees with the value for $b = 1.05 \pm 0.15$ in the fit of fig. 5.

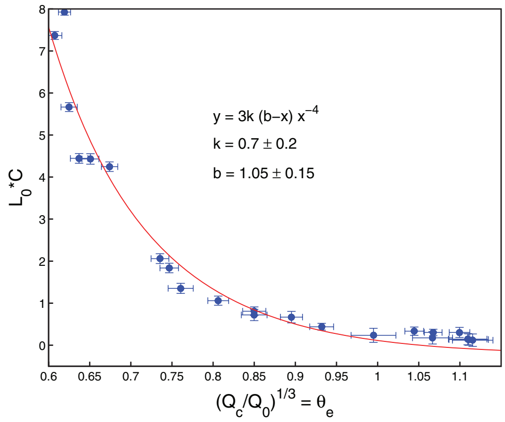

Fig. 5: (Colour on-line) Data of fig. 3 plotted as non-dimensional quantities using eq. (5). Note that the axes are exchanged with respect to fig. 3. L_0 and Q_0 are, respectively, a typical length and flow rate, they both depend on the width of the rivulet $2a$. C is the standard deviation of the curvilinear curvature and is a measure of the roughness of the contact line. Q_c is the critical rate of meandering. The continuous line corresponds to the fit equation (8), modeling the critical rate as the rate where the contact angle reaches its static limit.

Conclusion. – These experiments highlight the role played by the geometry of the contact line (and the wetting hysteresis) in the meandering instability. We showed that the critical rate of instability strongly depends on initial conditions through two parameters: the width of the rivulet and the roughness of the contact line (quantitatively measured by the RMS curvature). On the one hand, rough contact lines prevent the rivulet from flowing straight along the direction of steepest descent. Forced to flow along a constrained and perturbed path, the liquid experiences inertial forces which will deform the rivulet from its symmetric equilibrium shape. The perturbations will start to grow when the contact lines become mobile, that is when the deformation is such that the contact angle reaches its limit static value. The rougher the contact lines, the stronger the centrifugal forces, the stronger the deformation, and the smaller the critical flow rate. The initial width of the rivulet, on the other hand, fixes the contact angle at the equilibrium symmetric shape. The bigger the width, the smaller that contact angle, the bigger the distance to the critical contact angle, and therefore the higher the critical flow rate.

A model taking into accounts the two effects of initial width and contact line roughness fits the experimental measurements remarkably well, collapsing different initial conditions on a single curve (fig. 5).

Contact line pinning fundamentally changes the nature of the meandering instability, by introducing a finite threshold force for contact line movement. While the instability has previously been shown to be linear in the absence of pinning [12], pinning suppresses the sensitivity to infinitesimal perturbations. Small perturbations merely lead to changes in the rivulet cross-sectional shape, without any movement of contact lines, and this deformation is attenuated downstream by viscosity. A finite perturbation is thus required to produce a contact line movement. We showed that this threshold perturbation strongly depends on the preparation of the experiment. This is in stark contrast to the total wetting case, where the threshold is well defined independently of initial conditions.

Le Grand-Piteira *et al.* [9] always started from zero flow rate when measuring the critical flow rate for meandering. It seems likely to us that other reports of well-defined meandering thresholds also systematically interrupted the flow in between two measurements in order to obtain reproducible results. The measurements by Birnir *et al.* [13], on the other hand, may have been performed in different conditions. They observe meandering only when introducing flow rate fluctuations at the injection, and claim that the meanders disappear when switching back to a steady flow rate. However, they do observe cases of stationary meanders (see [13], p. 405), but dismiss these as due to dust, because cleaning the surface and re-starting the experiment produces a straight rivulet. The crucial of these two actions may however not be the cleaning of the surface, but the re-starting at the same flow rate. In our terms, this amounts to using a different preparation flow rate, and it is perfectly possible to produce a fresh straight rivulet at flow rates at which rivulets created at lower flow rates already start meandering. Meandering appears to be a metastable dynamics, co-existing with a straight rivulet dynamics at any given flow rate.

Considering that the critical flow rate for meandering increases as the rivulet is made smoother, one can ask whether this critical flow rate can be arbitrarily high, or whether there exists an upper limit for the instability threshold. In our model, we consider that the meandering threshold appears as soon as the contact line of the external side of a small perturbation reaches the limit contact angle and moves. This will happen at a finite flow rate even for a perfectly straight initial rivulet: by increasing the flow rates, we will increase the contact angles, both equal to θ_s (perfectly symmetric profile). At a flow rate of $Q_c = Q_0\,\theta_a^3$ (Q_0 is the characteristic flow rate depending only on the rivulet width) the contact angles will be equal to the limit advancing contact angle, and contact lines will move. At that point any perturbation due to wetting imperfections of the substrate will grow into meanders. For a given preparation flow rate, there is therefore always a critical meandering flow rate.

The critical flow rates of meandering in partial wetting conditions depend on the behavior of a rivulet submitted to an external force (centrifugal force here). In order to better understand the behavior of liquid rivulets, we therefore plan to analyse the response of the fluid flow to perturbations imposed by the contact line shape in more detail.

* * *

The authors thank L. Limat for discussions.

REFERENCES

[1] Leopold L. and Wolman M., *Geol. Soc. Am. Bull.*, **71** (1960) 769.

[2] Seminara G., *J. Fluid Mech.*, **554** (2006) 271.

[3] Camporeale C., Perona P., Porporato A. and Ridolfi L., *Rev. Geophys.*, **45** (2007) RG1001.

[4] Culkin J. and Davis S., *AIChE J.*, **30** (1984) 263.

[5] Bruinsma R., *J. Phys. (Paris)*, **51** (1990) 829.

[6] Young G. and Davis S., *J. Fluid Mech.*, **176** (1987) 1.

[7] Schmuki P. and Laso M., *J. Fluid Mech.*, **215** (1990) 125.

[8] Birnir B., Mertens K., Putkaradze V. and Vorobieff P., *Phys. Rev. Lett.*, **101** (2008) 114501.

[9] Le Grand-Piteira N., Daerr A. and Limat L., *Phys. Rev. Lett.*, **96** (2006) 254503.

[10] Nakagawa T., *Int. J. Multiphase Flow*, **18** (1992) 455.

[11] Drenckhan W., Gatz S. and Weaire D., *Phys. Fluids*, **16** (2004) 3115.

[12] Daerr A., Eggers J., Limat L. and Valade N., *Phys. Rev. Lett.*, **106** (2011) 184501.

[13] Birnir B., Mertens K., Putkaradze V. and Vorobieff P., *J. Fluid Mech.*, **607** (2008) 401.

[14] Nakagawa T. and Scott J. C., *J. Fluid Mech.*, **149** (1984) 89.